# Influence of Linker Molecules on Interfacial Electron Transfer and Photovoltaic Performance of Quantum Dot Sensitized Solar Cells

Junwei Yang[†], Takuya Oshima[‡], Witoon Yindeesuk[‡], Zhenxiao Pan[†], Xinhua Zhong[†,*], and Qing Shen[‡,§,*]

[†]Key Laboratory for Advanced Materials, Institute of Applied Chemistry, East China University of Science and Technology, Shanghai 200237, China

[‡]Department of Engineering Science, the University of Electro-Communications, 1-4-1 Chofugaoka, Chofu, Tokyo 182-8585, Japan

[§]Japan Science and Technology Agency (JST), 4-1-8 Honcho Kawaguchi, Saitama 332-0012, Japan

Email: zhongxh@ecust.edu.cn (for Z. X.); shen@pc.uec.ac.jp (for S. Q.)

## Abstract

Charge transfer rate between QD sensitizer/$TiO_2$ interfaces in quantum dot sensitized solar cells (QDSCs) is one of the most important criteria determining photovoltaic performance of cells. To investigate the influence of linker molecules on the electron transfer rate at QD-linker-$TiO_2$ interface and the final performance of the resultant QDSCs, colloidal QDs capped with thioglycolic acid (TGA), 3-mercaptopropionic acid (MPA), and cysteine (Cys), which also serve as molecular linkers between QD and $TiO_2$ nanoparticles, were self-assembled on $TiO_2$ mesoporous film electrode from corresponding QD aqueous dispersions. The influence of the studied linker molecules (TGA, MPA, Cys) on the loading amount of QD sensitizer on $TiO_2$ mesoporous film, the electron injection rate from QD to $TiO_2$ matrix, the incident photon to charge carrier generation efficiency (IPCE), and the corresponding photovoltaic performance of the resultant QDSCs were systematically studied. CdSe and $CdSe_xTe_{1-x}$ QD sensitized solar cells were selected as a model cell to evaluate the influence of the adopted linker molecules. Under AM 1.5G one full sun intensity illumination, the power conversion efficiency (PCE) of TGA-capped QDs (5.40% for CdSe, and 6.68% for $CdSe_xTe_{1-x}$) was 7-14% greater than those for MPA- and Cys-capped QDs. Similarly, the absorbed photon-to-current efficiency was 8-13% greater. These differences arise from linker molecule-dependent variations of electron-injection rate. Transient grating measurements indicate that electron injection rate constant from TGA-capped CdSe ($8.0 \times 10^9 \, s^{-1}$) was greater than from MPA- and Cys-capped CdSe ($2.6$-$2.9 \times 10^9 \, s^{-1}$). Thus, TGA-capped QDs are readily attached to $TiO_2$ substrate and exhibit better electronic properties and desirable electron-transfer rate, therefore bring forward better photovoltaic performance in the resultant solar cells.

# 1. Introduction

Quantum dot sensitized solar cells (QDSCs) constitute one of the most promising low cost candidates for the third-generation photovoltaic cells due to the various advantages of QD sensitizers in comparison with the conventional molecular dye sensitizers, such as the possibility of multiexciton generation (MEG), low-cost and ease of preparation, high molar extinction coefficient, size and composition tunable band gap, and large intrinsic dipole moment etc.[1-4] However, at present, the reported best power conversion efficiency of liquid-junction QDSCs (6-7%),[5-8] lags far behind their analogue dye sensitized solar cells (DSCs, up to 12%).[9] Partial reasons for this mean performance of QDSCs could be ascribed to the slow electron injection rate from QD to oxide matrix, since it is one of the most important criteria determining the cell photovoltaic performance.[10,11]

It is well recognized that the rate of electron injection from QDs to wide band gap metal oxide (mainly $TiO_2$, ZnO, or $SnO_2$) matrix/conductor is directly related to the way how the QD sensitizers are tethered on metal oxide. Usually, two general approaches have been developed for tethering QDs onto metal oxide electrodes: (i) direct growth of QDs onto oxides by chemical bath deposition (CBD), or successive ionic layer adsorption and reaction (SILAR) technique;[8,12-21] (ii) post-synthesis assembly using pre-synthesized colloidal QDs via direct adsorption, linker assisted assembly, or electrophoretic deposition (EPD) route.[5-7, 22-30] In the first approach, QD sensitizer (electron donor) contacts directly with oxide matrix (electron acceptor), therefore favoring the excited electron injection from QD into oxide matrix. While the surface passivation of QDs is difficult to control in this approach, the accompanied high density trap defect states together with the bare surface of QD create significant recombination centers, which would detrimentally affect the photovoltaic performance of the resulting cell devices.[10,11] These drawbacks can be effectively avoided by the second approaches using pre-prepared colloidal QDs, since the size, size distribution, shape, and surface functionalization, and consequently, the band gap alignment and optoelectronic properties, the density and energy of their trap states of colloidal QDs can be easily tailored and well controlled via the well-developed organometallic high temperature synthetic method.[10,11,31-33] More importantly, the existing bottleneck for the post-synthesis assembly approach, low loading of QD sensitizer on oxide matrix, has been effectively overcome by our recently developed *ex situ* ligand exchange self-assembly route with use of 3-mercaptopropionic acid (MPA) capped water-soluble QDs.[5-7,34,35] In this route a series of high-quality colloidal QDs have been immobilized uniformly throughout the photoanode film

thickness with up to 34% coverage.[35] More importantly, PCE of 5.32-7.04%, have been obtained in these resultant QDSCs through the use of this general deposit technique.[5-7,34,35]

Although our previous research has demonstrated that MPA-capped QD can be effectively tethered on TiO$_2$ film electrode with high loading and effective electron injection from QD to TiO$_2$,[5-7,34,35] there is no system study on the influence of different linker molecules on the electron injection rate and the accompanied photovoltaic performance of the resultant cell devices. Our investigation of the effect of different linker molecules was motivated by the recent theoretic and experimental results, which provide compelling evidence that the nature and especially the linker molecule chain length can significantly influence the electron injection rate and the performance of QDSCs.[22,26,31,32,36-45] According to Marcus theory, electron transfer rate is related directly with the electronic coupling strength, which is expected to decay exponentially with increasing separation between donor and acceptor.[46] This assumption has been verified by experimental results that both the electron injection rate and accompanied photovoltaic performance decreased dramatically with increasing alkyl chain length in mercaptoalkonic acid (MAA) linker molecules.[26,36,42,45] Mora-Seró et al. reported that the cell efficiency with use of thioglycolic acid (TGA) linker is higher (about double) compared to that for MPA and the corresponding reason was ascribed to the reduced tunnelling probability in MPA due to the longer separation distance, leading to the observed decrease of electron injection.[26] Watson and coworkers have characterized electron injection from CdS QD to TiO$_2$ nanoparticles as a function of the interparticle separation within molecularly linked assemblies and demonstrated that the electron injection yield decreased with increasing MAA chain length and interparticle separation.[36] In the practical QDSC system, Kamat and co-workers reported that MPA is a better linker than TGA or mercaptohexadecanoic acid.[22] In a similar way, several groups observed that cysteine (Cys) as a linker gives rise to more efficient photoanodes than using TGA or MPA.[26,40,44] It seems that there is somewhat confusion on the determination of optimum linker molecule. It should be highlighted that in most of the above mentioned linker-assisted post-synthesis assembly route for tethering QD sensitizer on oxide matrix, it was achieved by an *in situ* ligand exchange process, where TiO$_2$ films are first functionalized by the linker molecules followed by exposing to QD dispersions for QDs assembly. However this deposition route encounters problems with low QDs coverage, aggregation of QDs, poor reproducibility, and the resultant QDSCs show a relative poor PCE (usually < 2%).[10,11,31-33] Furthermore, most of the above mentioned transient kinetics investigations were limited to nanosecond time resolution but not

the picosecond time resolution,[36,37,40,41] which is impossible to probe electron transfer on the ultrafast time scale, the region that showcases the majority of temporal transient dynamics.
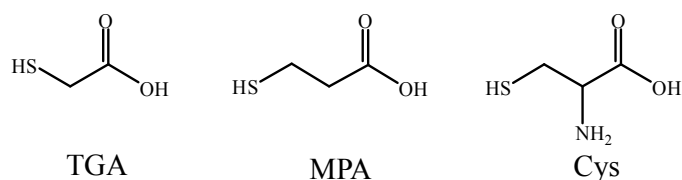


**Fig. 1** Molecular structure of studied bifunctional linker molecules

In this work, we focus on the investigation of the photovoltaic performance of QDSCs constructed by different linker molecules assisted assembly. For this purpose, we have analyzed CdSe, $CdSe_xTe_{1-x}$ based QDSCs, choosing the most common used phase transfer agents with structural similarity as shown in Fig. 1, i.e. TGA, MPA, Cys as the linker molecules. We investigated the influence of the studied linker molecules on the loading amount of QD sensitizer on $TiO_2$ film and the electron injection rate from QD to $TiO_2$ matrix, and the accompanied incident photon to charge carrier generation efficiency (IPCE) and photovoltaic performance of the resulting cell devices. CdSe and $CdSe_xTe_{1-x}$ QD sensitized solar cell was selected as model cells to evaluate the influence of the adopted linker molecules. The model QDSCs were constructed by our developed *ex situ* ligand exchange post-synthesis assembly technique via self-assembly of corresponding linker molecules capped water-soluble QD on $TiO_2$ electrode. We focus on the relationship between linker molecules (ultrafast kinetics) and the ultimate photovoltaic performance of a complete device. We have applied a recently developed improved transient grating (TG) technique to investigate the ultrafast carrier dynamics (on the picosecond time scale) of photogenerated electrons injection from QD to $TiO_2$ substrate. Experimental results indicate that electron injection rate from TGA-CdSe to $TiO_2$ is faster than those from MPA- or Cys-QDs. Correspondingly, the photovoltaic performance of TGA-QD show the best performance of 5.40% (for CdSe cell) and 6.68% (for $CdSe_xTe_{1-x}$ cell) under full 1 sum illumination, respectively, which are among the best results in the studied QD sensitizers based QDSCs.

## 2. Experimental Section

### Chemicals

Oleic acid (90%), 3-mercaptopropionic acid (MPA, 98%), cysteine (Cys, 97%), and thioglycolic acid (TGA, 97%) were obtained from Alfa Aesar. 1-octadecene (ODE, 90%), trioctylphosphine (TOP, 90%), selenium powder (200 mesh, 99.99%), cadmium oxide (CdO, 99.99%), tellurium powder (200 mesh, 99.99%), and oleylamine (OAm, 95%) were purchased from Aldrich. All reagents were used as received without any further purification.

### Synthesis of CdSe QDs and CdSe$_x$Te$_{1-x}$ Alloy QDs

The initial oil-soluble OAm-capped CdSe QDs with particle size of 5.4 ± 0.4 nm as determined by TEM measurements and first excitonic absorption peak at 620 nm were prepared via the organic phase high temperature route according to a literature method with minor modification.[47] Typically, 0.4 mL of 1.0 M Se stock solution in TOP was mixed with 10.0 mL OAm, and the mixture was heated to 300 $^o$C under N$_2$ flow with stirring. Then, 1.0 mL of 0.4 M Cd stock solution, prepared by dissolving CdO in oleic acid and ODE (v/v, 1:1) at 250 $^o$C, was injected, and the reaction mixture was kept at 280 $^o$C for 10 min. The obtained CdSe QDs were purified by centrifugation and decantation with the addition of methanol.

The preparation of CdSe$_x$Te$_{1-x}$ alloyed QDs with particle size of 5.2 ± 0.4 nm as determined by TEM measurements and absorption edge at 800 nm was according to a literature method by directly heating the reaction mixture containing Cd, Se, and Te precursors from room temperature to a certain high temperature.[48] Briefly, 0.1 M Te and Se stock solutions (obtained by dissolving Se or Te powder in TOP and paraffin (v/v, 1:3)),  0.1 M Cd precursor solution (obtained by dissolving CdO in oleic acid and paraffin (v/v, 1:3)) were loaded in a three-neck flask with a Cd:Te:Se molar ratio of 10:1:1. The mixture was then heated to 320 $^o$C under N$_2$ atmosphere and kept at this temperature for 10 min, followed by the addition of 2.0 mL of OAm into the reaction system and stayed for another 8 min at 260 $^o$C. The procedure for isolation and purification of the obtained CdSe$_x$Te$_{1-x}$ QD were the same as those for CdSe QDs as described above. The optical properties and TEM images of the obtained CdSe QDs and CdSe$_x$Te$_{1-x}$ QDs were available in Fig. S1† of the Electronic

Supplementary Information (ESI†).

**Preparation of Linker Molecule (TGA, MPA, and Cys) Capped Water Soluble QDs**

The water-soluble QDs were prepared via ligand exchange route according to a literature method.[5-7,49] Typically, 2.0 mmol of TGA, MPA, or Cys phase transfer agent (i.e. linker molecule) was first dissolved in 1.0 mL of methanol, and then pH of the solution was adjusted to 11 with use of 30% NaOH aqueous solution. 30 mL of the purified CdSe quantum dots dispersion in $CH_2Cl_2$ (containing CdSe QD 0.4 mmol) was equally divided into three portions. To each CdSe QD dispersion, the phase transfer agent solution was added and stirred for 2h to get the precipitation of QDs. Then the linker molecule capped CdSe QDs were extracted from $CH_2Cl_2$ solution by adding 10.0 ml deionized water. The CdSe QDs aqueous dispersion was further purified by centrifugation and decantation with the addition of acetone, and the precipitate re-dissolved in 2.0 ml deionized water. The PH of the obtained CdSe aqueous solution was adjusted to 11.0 for use in next step. Similarly, TGA-, MPA-, or Cys-capped water-soluble $CdSe_xTe_{1-x}$ QDs were prepared with the same procedure.

**Fabrication of QD-Sensitized Photoanodes and Solar Cells**

The photoanodes consist of double layer $TiO_2$ mesoporous film (i.e. transparent layer and light-scattering/opaque layer) coated on fluorine doped $SnO_2$ (FTO, 8 Ω/square) glass substrates.[50] Before the coating of $TiO_2$ film, the cleaned FTO glass was treated at 70 °C for 30 min with 40 mM $TiCl_4$ aqueous solution for the formation of a compact $TiO_2$ layer on the FTO substrate. The transparent layer (9.0 ± 0.5 μm) was then coated on the FTO substrate by successive screen-printing a home-made P25 paste, followed by a 6.0 ± 0.5μm thick light scattering layer with use of paste containing 200-400 nm sized $TiO_2$ particles. The electrodes were finally sintered at 500 °C for 15 min in a muffle-type furnace.

The QD sensitizers were immobilized on the $TiO_2$ mesoporous films by pipetting 30 μL of linker molecules capped QD aqueous dispersion onto the film surface and staying for 2-4 h before rinsed sequentially with water and ethanol and then dried with pressed air. After finishing deposition, the QD sensitized $TiO_2$ films were coated with ZnS by four times dipping alternately into 0.1 M $Zn(OAc)_2$ and 0.1 M $Na_2S$ solutions for 1 min/dip.

To prepare $Cu_2S$/brass counter electrode, brass foil was immersed in HCl solution (1.0 M) at 70 °C for 5 min and subsequently soaked into polysulfide electrolyte solution for 10 min. The polysulfide electrolyte solution was composed of $Na_2S$ (2.0 M), S (2.0 M), and KCl (0.2 M) in deionized water. The cell devices were constituted by assembling $Cu_2S$ counter electrode and QD-sensitized photoanode by a binder clip and injecting 10 μL of electrolyte.

**Characterization**

The UV/vis absorption spectra and the PL emission spectra were measured using a UV-visible spectrophotometer (Shimadzu UV-3101 PC) and a fluorescence spectrophotometer (Cary Eclipse Varian), respectively. Transition electron microscopy (TEM) images were obtained on a JEOL JEM-2100 microscope with accelerating voltage of 200 kV. Current-voltage characteristics (*J–V* curves) of QDSCs were measured using a Keithley 2400 source meter and an AM 1.5G solar simulator (Oriel, Model No.94022A) provided simulated illumination at intensity of 100 mW/cm$^2$. Photoactive area was 0.237 cm$^2$, which was defined by a black plastic disk. Incident photon-to-current conversion efficiency (IPCE) spectrum was measured using a Keithley 2000 multimeter, and a spectral product DK240 monochrometer with 300 W tungsten lamp provided illumination. Electron injection rate from the QDs to $TiO_2$ electrodes through different linker molecules were characterized using an improved transient grating (TG) technique. The principle of the improved TG method has been explained in detail.[51-53] The laser source was a titanium/sapphire laser (CPA-2010, Clark-MXR Inc.) with a wavelength of 775 nm, a repetition rate of 1 kHz, and a pulse width of 150 fs. The light was separated into two parts. Half of it was used as a probe pulse. The other half of the light was used to pump an optical parametric amplifier (OPA) (a TOAPS from Quantronix) to generate light pulses with a wavelength tunable from 290 nm to 3 μm; used as a pump light in the TG measurement. In this study, the experiment was carried out under $N_2$ environment, and under excitation wavelength of 620 nm. The probe light wavelength is 775 nm. The typical laser pulse intensity used in the TG experiments was as low as 2 mW. The area of the laser beam on the sample was about 0.2 cm$^2$. The samples showed no apparent photo-damage during the TG measurements.

## 3. Results and Discussion

In order to evaluate the influence of different linker molecules on the photovoltaic performance of the resulting QDSCs and therefore determine the optimum linker molecule, CdSe and $CdSe_xTe_{1-x}$ QD sensitized $TiO_2$ photoanodes were obtained by the self-assembly of the studied linker molecules (i.e., TGA, MPA, and Cys) capped QD on mesoporous $TiO_2$ film photoanodes. All cell samples were constructed using polysulfide/sulfide aqueous solution as electrolyte and $Cu_2S$ as counter electrode and the photovoltaic performance was measured under standard conditions (100 mW/cm$^2$, AM 1.5G). The selection of CdSe and $CdSe_xTe_{1-x}$ QD sensitizers is due to their facile and well-developed synthetic method, relatively broad light-harvesting range, and the satisfied photovoltaic performance of the resulting QDSCs.[5,35] The synthesis of oil-soluble oleylamine-capped CdSe (average 5.4 nm sized with first excitonic absorption peak at 620 nm) and $CdSe_xTe_{1-x}$ QDs (average 5.2 nm sized with absorption edge at 800 nm), water-solubilization of the initial oil-soluble QDs into water-soluble linker molecules (TGA, MPA, or Cys) capped QDs, and the immobilization of water-soluble QDs onto $TiO_2$ film electrode followed our own recently developed literature methods,[5,35] and the detailed procedure were presented in the Experimental Section. Under each condition, average photovoltaic performance for at least five cells in parallel was analyzed.

**Influence of Cell Photovoltaic Performance by Linker Molecules**

Fig. 2 shows the representative *J-V* curves of the QDSCs with intermediate performance based on different linker molecules capped QD sensitizers. The extracted average photovoltaic parameters of every group of cells are summarized in Table 1, with details of each cell available in Table S1-2† of ESI†. From these data, we can find that the PCE values for both CdSe and $CdSe_xTe_{1-x}$ QDSCs based on different linker molecules show the same trend with TGA > MPA > Cys. The TGA linker based CdSe and $CdSe_xTe_{1-x}$ QDSCs exhibit the best PCE values of 5.40% and 6.68%, respectively. Furthermore, the enhanced PCE for TGA based cells are mainly benefited from the improved short-circuit density ($J_{sc}$), while the open-circuit voltage ($V_{oc}$) and fill factor (FF) for the corresponding cells are nearly independent on the linker molecules. We can therefore conclude that TGA serving as the linker molecule has the best photovoltaic performance for the QDSCs fabricated by *ex situ* ligand exchange post-synthesis assembly approach. This conclusion is contrary to most of the previous results, where Cys based QDSCs shows the best photovoltaic performance.[26,40,44] It

should be noted that in most of these reports, the pre-prepared colloidal QD sensitizers were tethered on TiO$_2$ matrix via *in situ* ligand exchange process, and the resultant QDSCs all show a relative poor PCE (usually < 2%) regardless whichever linker molecules used.
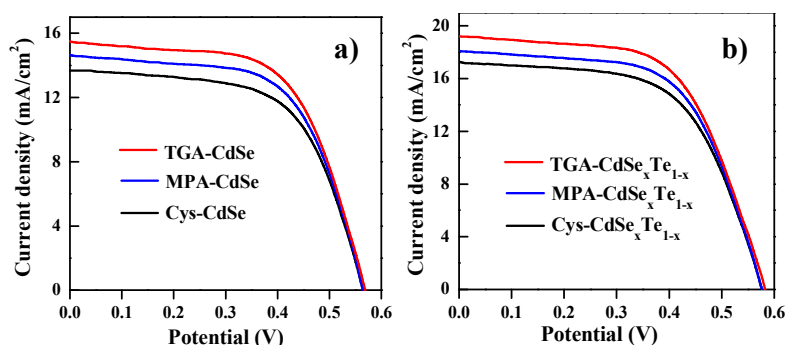


**Fig. 2** The representative *J-V* curves of TGA-, MPA-, and Cys-capped CdSe (a) and CdSe$_x$Te$_{1-x}$ (b) QDs based QDSCs, respectively.

**Table 1 Photovoltaic Parameters for QDSCs Based on Different Linker Molecules Capped CdSe and CdSe$_x$Te$_{1-x}$ QDs Sensitizers.**

| QDs | linker | $J_{sc}$ (mA·cm$^{-2}$) | $V_{oc}$ (V) | FF (%) | PCE (%)[a] |
|---|---|---|---|---|---|
| | TGA | 15.48 | 0.568 | 0.612 | 5.40±0.04 |
| CdSe | MPA | 14.63 | 0.566 | 0.611 | 5.06±0.05 |
| | Cys | 13.68 | 0.565 | 0.612 | 4.72±0.07 |
| | TGA | 19.20 | 0.583 | 0.596 | 6.68±0.06 |
| CdSe$_x$Te$_{1-x}$ | MPA | 18.11 | 0.580 | 0.599 | 6.33±0.07 |
| | Cys | 17.27 | 0.577 | 0.598 | 5.95±0.06 |

[a] average value with standard deviation based on 5 cell devices in parallel.

Hereafter, CdSe QD based solar cells were chosen to further study the influence of cell photovoltaic performance by linker molecules. Fig. 3a shows the absorption spectra of TGA-, MPA-, and Cys-capped CdSe QDs sensitized TiO$_2$ films with identical configuration and film thickness, and the corresponding photographs are shown in the inset. The absorption peaks of all the sensitized films are located at the same wavelength around 620 nm, and this indicates that no particle aggregation has happened. Since the absorbance is directly related to the amount of QD sensitizer uploaded, we can find that that the loading amount of CdSe QDs

follows the order of TGA > MPA > Cys from the absorption spectra, which is consistent with the trend of PCE and $J_{sc}$ of the resultant cell devices as described above. Obviously, higher loading of QD sensitizers on photoanodes can harvest more incident solar photons and achieve higher photocurrent, therefore the observed different loading amounts can partially explain the different $J_{sc}$ values among TGA-, MPA- and Cys-QD based cell devices.
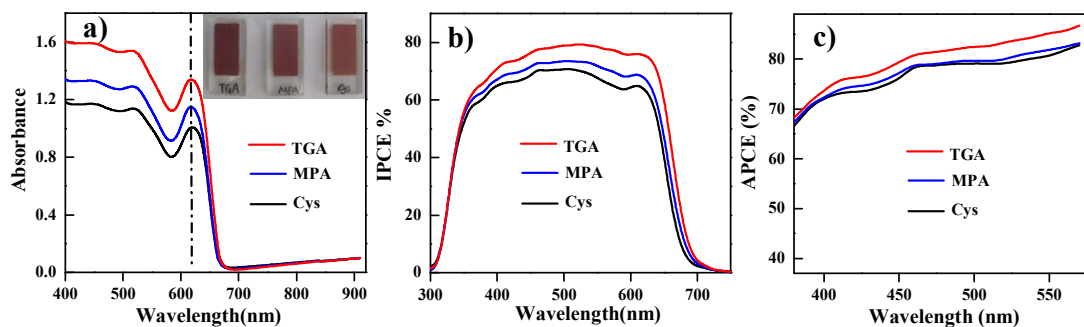


**Fig. 3** Absorption spectra (a) of TGA-, MPA-, and Cys-capped CdSe $QD_{620}$ sensitized $TiO_2$ films. Inset: photographs of films sensitized by different molecules linked CdSe. IPCE curves (b) and APCE curves (c) for every kind of CdSe QDSCs, respectively.

To further exploit the causes of the obtained different $J_{sc}$ value, the incident-photo-to-carrier conversion efficiency (IPCE, i.e. external quantum yield, EQE) was measured in accordance with conversion efficiency of monochromatic light irradiation and shown in Fig. 3b. The IPCE responses show a similar spectral profile with the identical photoresponse range for three different cells devices, and the highest IPCE values for the TGA-, MPA-, and Cys-CdSe QDSCs are 79.4, 73.4, and 70.7%, respectively. In the whole light response range, the IPCE values for CdSe QDSCs based on different linker molecules follow the order of TGA > MPA > Cys, which is consistent with that of corresponding $J_{sc}$ values. But we cannot directly make a conclusion that the electron collection and/or injection efficiency of TGA based cells is higher than those of MPA and Cys based ones, since the IPCE values depend on a series of device parameters: IPCE = LHE $\times \phi_{inj} \times \eta_{cc}$, where LHE is the light harvesting efficiency, $\phi_{inj}$ is the electron injection efficiency, and $\eta_{cc}$ is charge collection efficiency. To examine more accurately the electron collection and/or injection efficiency for different linker molecules based sensitizers, the APCE (absorbed photon to electron conversion efficiency) was calculated according to the following equation of APCE($\lambda$) = IPCE($\lambda$)/[1-10^{-Abs($\lambda$)}],[54] where Abs($\lambda$) is the absorbance of photoanode at wavelength $\lambda$, and the results are shown in Fig. 3c. This takes out the effect of varying optical densities of the

different electrodes. We can see that the APCE values corresponding to TGA based cells are still higher than that of MPA and Cys based cells in the whole light-response range, but the difference become lesser in comparison with those of IPCE. This clearly demonstrates that the electron collection and/or injection efficiency of the TGA based cells are higher than that of MPA and Cys based cells. Since these cells with the analogous configuration have the similar $\eta_{cc}$,[54] the difference of $\phi_{inj}$ should be the dominant factor that impacts the APCE values, which is supported by *J-V* curves under dark condition of QDSCs (Fig. S2†) based on the studied three linker molecules (TGA, MPA, and Cys) displaying nearly identical curves with similar photovoltage onset and dark current value. This indicates that the electron injection is less efficient for the MPA- and Cys-capped CdSe QD sensitizers than the TGA-capped QD sensitizer, and the $\phi_{inj}$ of MPA-CdSe and Cys-CdSe is almost coincident. Therefore, higher coverage of QDs and higher electron injection efficiency at QDs-linker-TiO$_2$ interface resulted in higher $J_{sc}$ of TGA-CdSe sensitized solar cells. The observed different $J_{sc}$ values for MPA and Cys based cell devices should be ascribed to the different loading amounts of QD sensitizers on TiO$_2$ photoanode as shown in Fig. 3a. Comparing to MPA and Cys, we speculate that TGA can increase electron injection efficiency from QDs to TiO$_2$ matrix due to reduce the chain length by one sp$^3$ hybridized C element.
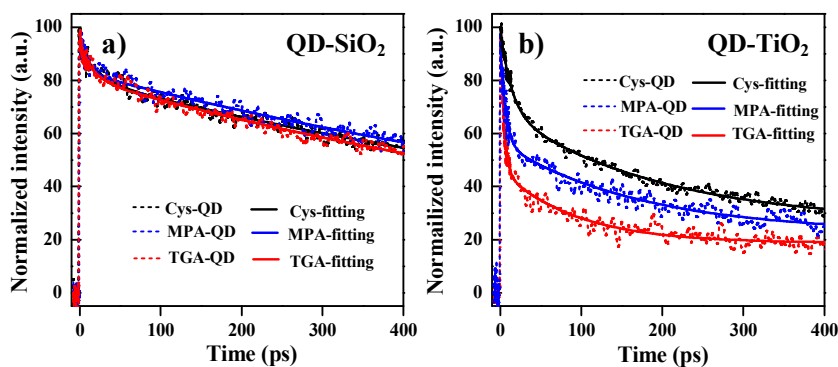


**Fig. 4** TG responses (dashed lines) of TGA-, MPA-, Cys-capped CdSe QDs deposited on SiO$_2$ (a), and on TiO$_2$ (b) nanoparticle substrate. The solid lines represent the corresponding bi-exponential fit.

## Ultrafast Carrier Dynamics Study

To further characterize effects of the different linker molecules on the electron injection process from the QDs to TiO$_2$, we employed the improved transient grating (TG) technique to measure the photoexcited carrier relaxation dynamics in QDs deposited on insulating SiO$_2$ or

TiO$_2$ films through the three kinds of linker molecules. As explained in previous papers in detail,[51-53] the TG decay provides a direct measurement of free electron and hole carrier dynamics in QDs. The experimental results are shown in Fig. 4. In the case of QDs on SiO$_2$, there is no electron transfer from QDs to SiO$_2$ due to the conduction band of SiO$_2$ is much higher than that of the QDs. As shown in Fig. 4a, when QDs deposited onto SiO$_2$, there are only radiative and nonradiative recombination of charge carriers that contribute to the TG decay, so the three linkers capped CdSe QDs have almost the same decay curves. However, for QDs on TiO$_2$, photo-generated electrons in the QDs can inject into TiO$_2$ since the conduction band edge of TiO$_2$ is lower than that of QDs. As shown in Fig. 4b, a significant faster decay can be observed for QDs deposited on TiO$_2$ compared to those of QDs on SiO$_2$ through different linker molecules, indicating electron injection occurring at the QDs/TiO$_2$ interface which is an additional pathway to carrier relaxation in QDs. Biexponential decay function (*eq* 1) was found to fit very well with the TG response as shown in Fig. 4 and average lifetime ($\tau_{av}$) was then estimated based on the fitting results by using *eq* 2.

$$y = A_1 e^{-t/\tau_1} + A_2 e^{-t/\tau_2} + y_0 \qquad (1)$$

$$\tau_{av} = \left(A_1\tau_1^2 + A_2\tau_2^2\right)/\left(A_1\tau_1 + A_2\tau_2\right) \qquad (2)$$

where $A_1$ and $A_2$ are weighted coefficients and $\tau_1$ and $\tau_2$ are the lifetime for the two exponential components, $y_0$ is a constant corresponding to a carrier relaxation component with much longer lifetime than the measured time scale in this experiment (i.e., 400 ps), respectively. The fitting results and calculated average lifetime ($\tau_{av}$) are listed in Table **2**.

**Table 2 Fitting Results of the TG Responses of CdSe QD Sensitized TiO$_2$ Films**

| Samples | $t_1$ (ps) | $t_2$ (ps) | $A_1$ | $A_2$ | $y_0$ | $\tau_a$ (ps) | $k_{et}$ ($\times 10^9$ s$^{-1}$) |
|---|---|---|---|---|---|---|---|
| TGA-QD-SiO$_2$ | 6.4 | 275.4 | 9.2 | 41.0 | 44.3 | 274.01 | |
| TGA-QD-TiO$_2$ | 4.1 | 92.2 | 50.1 | 27.7 | 18.7 | 85.7 | 8.0 |
| MPA-QD-SiO$_2$ | 5.0 | 305.6 | 10.4 | 38.8 | 47.6 | 304.3 | |
| MPA-QD-TiO$_2$ | 5.7 | 167.4 | 34.1 | 37.5 | 22.8 | 161.6 | 2.9 |
| Cys-QD-SiO$_2$ | 9.6 | 350.8 | 9.3 | 42.5 | 41.7 | 348.75 | |
| Cys-QD-TiO$_2$ | 13.6 | 192.6 | 30.1 | 42.8 | 26.2 | 184.2 | 2.6 |

By comparing the TG decay processes of the QDs on TiO$_2$ to those of QDs on SiO$_2$, we can calculate the rate constants of electron transfer ($k_{et}$) by the following *eq* 3:

$$k_{et} = 1/\tau_{av(TiO_2)} - 1/\tau_{av(SiO_2)} \qquad (3)$$

where $\tau_{av(TiO_2)}$ represents the average lifetime of QDs on $TiO_2$ film and $\tau_{av(SiO_2)}$ is the average lifetime of QDs on $SiO_2$. According to *eq 3*, we obtained electron injection rate ($k_{et}$) of $8.0\times10^9$, $2.9\times10^9$, $2.6\times10^9$ s$^{-1}$ for TGA-CdSe, MPA-CdSe, and Cys-CdSe, respectively. It is noted that our observed $k_{et}$ value by the TG measurement is in the same level as obtained via transient absorption previously.[23] Electron injection rate of TGA-CdSe is distinctly higher than those of MPA-CdSe and Cys-CdSe. This observation also confirms that TGA, reducing the length of chain by one sp$^3$ hybridized C element, prefers to electron transfer compared to MPA and Cys. The higher electron injection rate will contribute to higher IPCE value and higher short circuit current, and actually this has been demonstrated in the former section.

## 4. Conclusions

In summary, TGA, MPA, Cys as capping ligand around QD and as linker molecules in immobilization of QD sensitizer on $TiO_2$ photoanode were investigated on the influence of the electron injection from QD to $TiO_2$ matrix and the photovoltaic performance of the resultant solar cells. The photovoltaic performance of TGA-QD show the best results of 5.40% (for CdSe cell) and 6.68% (for $CdSe_xTe_{1-x}$ cell) under full 1 sum illumination, respectively. The enhanced PCE for TGA based QDSCs are mainly benefited from the improved short-circuit density ($J_{sc}$), and the increase of $J_{sc}$ is based on: i) TGA-capped QD can boost the electron transfer rate and accompanied electron injection efficiency ($\phi_{inj}$) from QD to $TiO_2$ as illustrated by TG measurement and APCE characterization; and ii) comparing to MPA- and Cys-QD, TGA-QD provides a higher loading on $TiO_2$ film, which harvests more incident solar photons. The obtained results open up a new way to improve the photovoltaic performance of QDSCs.

## Acknowledgements

† Electronic Supplementary Information (ESI) available: Optical properties of as-prepared oil-soluble CdSe and CdSe$_x$Te$_{1-x}$ QDs dispersions, TEM images of as-prepared CdSe and CdSe$_x$Te$_{1-x}$ QDs, detail photovoltaic parameters for 5 QDSCs in parallel based on different link-molecules capped CdSe and CdSe$_x$Te$_{1-x}$ QDs sensitizers.

# References

1 I. J. Kramer and E. H. Sargent, *Chem. Rev.*, 2014, **114**, 863−882.

2 P. V. Kamat, K. Tvrdy, D. R. Baker and J. G. Radich, *Chem. Rev.*, 2010, **110**, 6664–6688.

3 J. B. Sambur, T. Novet and B. A. Parkinson, *Science*, 2010, **330**, 63−66.

4 O. E.Semonin, J. M. Luther, S. Choi, H.-Y. Chen, J. Gao, A. J. Nozik and M. C. Beard, *Science*, 2011, **334**, 1530−1533.

5 Z. Pan, K. Zhao, J. Wang, H. Zhang, Y. Feng and X. Zhong, *ACS Nano*, 2013, **7**, 5215–5222.

6 J. Wang, I. Mora-Seró, Z. Pan, K. Zhao, H. Zhang, Y. Feng, G. Yang, X. Zhong and J. Bisquert, *J. Am. Chem. Soc.*, 2013, **135**, 15913−15922.

7 Z. Pan, I. Mora-Seró, Q. Shen, H. Zhang, Y. Li, K. Zhao, J. Wang, X. Zhong and J. Bisquert, *J. Am. Chem. Soc.*, 2014, **136**, 9203–9210.

8 K. Yan, L. Zhang, J. Qiu, Y. Qiu, Z. Zhu, J. Wang and S. Yang, *J. Am. Chem. Soc.*, 2013, **135**, 9531–9539.

9 A. Yella, H. W. Lee, H. N. Tsao, C. Yi, A. K. Chandiran, M. K. Nazeeruddin, E. W. Diau, C. Yeh, S. M. Zakeeruddin and M. Grätzel, *Science*, 2011, **334**, 629–634.

10 I. Mora-Seró, S. Giménez, F. Fabregat-Santiago, R. Gómez, Q. Shen, T. Toyota and J. Bisquert, *Acc. Chem. Res.*, 2009, **42**, 1848–1857.

11 G. J. Hodes, *Phys. Chem. C*, 2008, **112**, 17778–17787.

12 Md. A. Hossain, J. R. Jennings, C. Shen, J. H. Pan, Z. Y. Koh, N. Mathews and Q. Wang, *J. Mater. Chem.*, 2012, **22**, 16235–16242.

13 Q. Zhang, X. Guo, X. Huang, S. Huang, D. Li, Y. Luo, Q. Shen, T. Toyoda and Q. Meng, *Phys. Chem. Chem. Phys.*, 2011, **13**, 4659–4667.

14 X. Yu, B. Lei, D. Kuang and C. Su, *J. Mater. Chem.*, 2012, **22**, 12058–12063.

15 H. Lee, M. Wang, P. Chen, D. R. Gamelin, S. M. Zakeeruddin, M. Grätzel and Md. K. Nazeeruddin, *Nano Lett.*, 2009, **9**, 4221–4227.

16 H. J. Lee, J. Bang, J. Park, S. Kim and S. M. Park, *Chem. Mater.*, 2010, **22**, 5636–5643.

17 H. Wang, C. Luan, X. Xu, S. V. Kershaw and A. L. Rogach, *J. Phys. Chem. C*, 2012, **116**, 484–489.

18 L. Li, X. Yang, J. Gao, H. Tian, J. Zhao, A. Hagfeldt and L. Sun, *J. Am. Chem. Soc.*, 2011, **133**, 8458–8460.

19 P. K. Santra and P. V. Kamat, *J. Am. Chem. Soc.*, 2012, **134**, 2508–2511.

20 J.-W. Lee, J.-D. Hong and N.-G. Park, *Chem. Commun.*, 2013, **49**, 6448–6450.

21 J.-W. Lee, D.-Y. Son, T. K. Ahn, H.-W. Shin, I. Y. Kim, S.-J. Hwang, M. J. Ko, S. Sul, H. Han and N.-G. Park, *Sci. Rep.*, 2013, **3**, 1050.

22 I. Robel, V. Subramanian, M. Kuno and P. V. Kamat, *J. Am. Chem. Soc.*, 2006, **128**, 2385–2393.

23 A. Kongkanand, K. Tvrdy, K. Takechi, M. Kuno and P. V. Kamat, *J. Am. Chem. Soc.*, 2008, **130**, 4007–4015.

24 J. H. Bang and P. V. Kamat, *ACS Nano*, 2009, **3**, 1467–1476.

25 Z. Ning, H. Tian, C. Yuan, Y. Fu, H. Qin, L. Sun and H. Ågren, *Chem. Commun.*, 2011, **47**, 1536–1538.

26 I. Mora-Seró, S. Giménez, T. Moehl, F. Fabregat-Santiago, T. Lana-Villareal, R. Gómez and J. Bisquert, *Nanotechnology*, 2008, **19**, 424007.

27 P. Sheng, W. Li, J. Cai, X. Wang, X. Tong, Q. Cai and C. A. Grimes, *J. Mater. Chem. A*, 2013, **1**, 7806–7815.

28 A. Salant, M. Shalom, I. Hod, A. Faust, A. Zeban and U. Banin, *ACS Nano*, 2010, **4**, 5962–5968.

29 H. McDaniel, N. Fuke, N. S. Makarov, J. M. Pietryga and V. I. Klimov, *Nat. Commun.*, 2013, **4**, DOI: 10.1038/ncomms3887.

30 P. K. Santra and P. V. Kamat, *J. Am. Chem. Soc.*, 2013, **135**, 877−885.

31 D. F. Watson, *J. Phys. Chem. Lett.*, 2010, **1**, 2299–2309.

32 N. Guijarro, T. Lana-Villarreal, I. Mora-Seró, J. Bisquert and R. Gómez, *J. Phys. Chem. C*, 2009, **113**, 4208–4214.

33 J. B. Sambur, S. C. Riha, D. Choi and B. A. Parkinson, *Langmuir*, 2010, **26**, 4839–4847.

34 Z. Pan, H. Zhang, K. Cheng, Y. Hou, J. Hua and X. Zhong, *ACS Nano*, 2012, **6**, 3982−3991.

35 H. Zhang, K. Cheng, Y. Hou, Z. Fang, Z. Pan, W. Wu, J. Hua and X. Zhong, *Chem. Commun.*, 2012, **48**, 11235−11237.

36 R. S. Dibbell and D. F. Watson, *J. Phys. Chem. C*, 2009, **113**, 3139–3149.

37 R. S. Dibbell, D. G. Youker and D. F. Watson, *J. Phys. Chem. C*, 2009, **113**, 18643–18651.

38 N. Guijarro, Q. Shen, S. Gimenez, I. Mora-Seró, J. Bisquert, T. Lana-Villarreal, T. Toyoda and R. Gomez, *J. Phys. Chem. C*, 2010, **114**, 22352–22360.

39 D. R. Pernik, K. Tvrdy, J. G. Radich and P. V. Kamat, *J. Phys. Chem. C*, 2011, **115**, 13511–13519.

40 J. S. Nevins, K. M. Coughlin and D. F. Watson, *ACS Appl. Mater. Interfaces*, 2011, **3**, 4242−4253.

41 B. R. Hyun, A. C. Bartnik, L. F. Sun, T. Hanrath and F. W. Wise, *Nano Lett.*, 2011, **11**, 2126–2132.

42 H. Wang, E. R. McNellis, S. Kinge, M. Bonn and E. Canovas, *Nano Lett.*, 2013, **13**, 5311–5315.

43 D. A. Hines and P. V. Kamat, *J. Phys. Chem. C*, 2013, **117**, 14418–14426.

44 J. T. Margraf, A. Ruland, V. Sgobba, D. M. Guldi and T. Clark, *Langmuir*, 2013, **29**, 2434−2438.

45 H. J. Yun, T. Paik, M. E. Edley, J. B. Baxter and C. B. Murray, *ACS Appl. Mater. Interfaces*, 2014, **6**, 3721–3728.

46 R. A. Marcus, *J. Chem. Phys.*, 1956, **24**, 966–978.

47 X. Zhong, Y. Feng and Y. Zhang, *J. Phys. Chem. C*, 2007, **111**, 526–531.

48 L. Liao, H. Zhang and X. Zhong, *J. Lumin.*, 2011, **131**, 322–327.

49 L. Liu, X. Guo, Y. Li and X. Zhong, *Inorg. Chem.*, 2010, **49**, 3768–3775.

50 Z. Du, H. Zhang, H. Bao and X. Zhong, *J. Mater. Chem. A*, 2014, **2**, 13033–13040.

51 K. Katayama, M. Yamaguchi and T. Sawada, *Appl. Phys. Lett.*, 2003, **82**, 2775–2777.

52 Q. Shen, M. Yanai, K. Katayama, T. Sawada and T. Toyoda, *Chem. Phys. Lett.*, 2007, **442**, 89–96.

53 V. Gonzalez-Pedro, C. Sima, G. Marzari, P. P. Boix, S. Gimenez, Q. Shen, T. Dittrich and I. Mora-Seró, *Phys.Chem. Chem. Phys.*, 2013, **15**, 13835–13843.

54 A. Fillinger and B. A. Parkinson, *J. Electrochem. Soc.*, 1999, **146**, 4559–4564.

Table of Contents (TOC)

**Influence of Linker Molecules on Interfacial Electron Transfer and Photovoltaic Performance of Quantum Dot Sensitized Solar Cells**

Junwei Yang, Takuya Oshima, Witoon Yindeesuk, Zhenxiao Pan, Xinhua Zhong, and Qing Shen

The influence of linker molecules on the electron transfer rate and photovoltaic performance of the resultant QDSCs has been investigated